UCRL-2237
Unclassified-Physics Distribution

UNIVERSITY OF CALIFORNIA

Radiation Laboratory

Contract No. W-7405-eng-48

SCATTERING OF 190-MEV DEUTERONS ON PROTONS

Arnold L. Bloom and Owen Chamberlain

June 4, 1953

Berkeley, California

UCRL-2237
Unclassified-Physics Distribution

SCATTERING OF 190-MEV DEUTERONS ON PROTONS

Arnold L. Bloom* and Owen Chamberlain

Radiation Laboratory, Department of Physics,
University of California, Berkeley, California

June 4, 1953

I. INTRODUCTION

Nucleon-nucleon scattering experiments have long been considered of primary importance for the determination of the nature of nucleon-nucleon forces. We are mostly concerned at this time with high energy scattering, in particular neutron-proton and proton-proton scattering with laboratory energies of approximately 90 Mev.[1-5] It seems most reasonable to take the view that n-p and p-p scattering are both derivable from the same interaction. If so, then the n-p and p-p scattering experiments give two approaches to this interaction. (The Pauli principle operates to explain the difference between n-p and p-p scattering measurements by excluding certain spin-angular momentum states from the p-p scattering.)

It is to be expected that in neutron-deuteron or proton-deuteron scattering there will be interference effects between n-p and n-n (or p-p) scattering. Thus n-d or p-d scattering experiments should allow another approach to knowledge of the nucleon-nucleon interaction. It was in the hope of obtaining some measure of this interference that the present experiments on p-d scattering were undertaken.

The theory of n-d and p-d scattering has been studied in some detail by Wu and Ashkin[6], by Chew[7-9], and by Bethe and Gluckstern.[10] In the present paper we report measurement of the total d-p scattering cross section, and of some studies of those inelastic d-p scatterings in which both outgoing protons can be observed at significant angles from the beam direction. In the following paper[11] elastic d-p scattering will be studied.

---

* Present address: Varian Associates, Palto Alto, California.

II. METHOD

Our source of high energy deuterons was the external deuteron beam of the 184-inch Berkeley cyclotron. In this beam was placed either a hydrogenous target (polyethylene, $(CH_2)_n$), or a carbon target, and the particles scattered out of the beam were observed in scintillation counters. The counting rate due to hydrogen was determined by subtraction of carbon counts from those obtained with CH_2. The beam was monitored by means of an ionization chamber and electrometer. Sections IV and V describe measurements of the total d-p scattering cross section and the differential p-p type scattering cross section resulting from inelastic d-p collisions, respectively. Results are presented in Tables I and III, and in Fig. 8.

Except for minor changes, the handling of the deuteron beam in this work has been the same as that given the proton beam in the p-p scattering experiments of Chamberlain, Segrè, and Wiegand.[4] The beam is obtained in the same way from the cyclotron, is collimated in the same way, and monitored with the same ionization chambers. Virtually identical precautions have been observed. The calibration of the ionization chambers has been extended to 192 Mev deuterons with the help of the range-energy relations of Aron, Hoffman, and Williams.[12]

A block diagram of one of two possible electronic arrangements is shown in Fig. 1. The crystals were used in conjunction with 1P21 photomultipliers and distributed preamplifiers. The pulses were then amplified in distributed amplifiers, shaped by fast discriminators, and mixed in distributed coincidence circuits.[13] Thus it was possible to count single events in the two crystals, as well as coincidences between crystals 1 and 2. The pulses put out by the amplifiers had an approximate width of $2 \cdot 10^{-8}$ sec; those out of the discriminator were about three times as wide, and fairly square in shape. The coincidence circuits had a dead time of about 10^{-7} sec, and the scalers a resolving time of about 10^{-6} sec.

Two methods of operation were used. In method A, employed in Section V below, two crystals were used, one on each arm of the table, and their single counts and coincidences were recorded by a scaling circuit. In method B, employed in Section IV, a single crystal was used. The hydrogenous targets were sheets of commercial polyethylene $(CH_2)_n$. The carbon targets were of graphite machined to such a thickness that they offered about the same stopping power to 192 Mev deuterons as the CH_2 targets used in conjunction with them.

III. EXPERIMENTAL PROCEDURE

Adjustments of cyclotron parameters, the collimator, and the central axis of the scattering table were carried out in the fashion described by Chamberlain, Segrè, and Wiegand. The alignment was checked using photographic film.

In each run the final checks on alignment and tests of the counters were accomplished by a brief study of elastic d-p scattering at one angle. In such a coincidence measurement using two crystals A and B, and correlated angles, one crystal A was made "defining" by keeping its dimensions small while the other crystal B was made large enough and placed close enough so that all the partners of the correlated (elastic d-p) events counted by A were sure to be received in crystal B. The angle between the two counters was varied, keeping ϕ (angle of "defining" crystal) fixed. The hydrogen coincidence counting rate was then plotted as a function of Θ, the angle of the non-defining crystal from the beam. The location of the center of the peak in counting rate indicated the observation of the elastic d-p scattering and gave a further check on alignment and the scales on which angles were measured. With the counters set at the elastic d-p scattering angles the counter plateaus were studied. That is, the voltage of each photomultiplier was varied in turn, and the hydrogen coincidence rates were plotted as functions of each counter voltage. The plateau curves were in all cases similar to those obtained by Chamberlain, Segrè, and Wiegand, and are not shown in this paper.

Several times during the course of these experiments the energy of the deuteron beam was determined by finding its range in aluminum. This was accomplished by placing two ionization chambers in the beam with a variable aluminum absorber between them. In all cases the energy was found to be the same within experimental accuracy, namely 192 ± 2 Mev.

Before proceeding to the actual counting, the carbon subtraction factor had to be found. The coincidences $\underline{CH_2}$ from CH_2 were counted for unit integrated beam ("integrator volt"). The carbon target was then inserted and coincidences $\underline{C}$ from it were recorded for one integrator volt; similarly with the coincidences $\underline{b1}$ when no target was in the beam. If we call $\underline{H}$ the number of coincidence counts per integrator volt due to hydrogen, we have

$$\underline{H} = \underline{CH_2} - \underline{zC} - (1-z)\,\underline{b1} \qquad (1)$$

where z is the carbon subtraction factor. If we use method B (single crystal) the coincidence counts are replaced by single counts and clearly z = R, where R is the ratio of the surface density of carbon in the CH_2 target to the surface density of the carbon target. This equality does not hold for method A since in addition to the desired systematic coincidences from hydrogen we count with a CH_2 target (a) a background of accidental coincidences, (b) accidental coincidences from carbon, (c) systematic coincidences from carbon, (d) accidental "mixed" coincidences from (inelastic or elastic) hydrogen events arriving in one counter and carbon events in the other. z is now a function not only of R, but also of the duty cycle of the cyclotron, the photomultiplier voltages and discriminator settings, and the angles $\ominus$ and ϕ.

Several methods are available for determining the carbon subtraction factor z. The method used most extensively involves repeating one counting arrangement at several different beam levels. From these data one can evaluate the effective resolving time of the apparatus, which is essentially the electronic resolving time divided by the duty cycle of the cyclotron. When the effective resolving time has been determined, the factor z can be computed from a reasonably simple expression involving the single counting rates and coincidence counting rates from the various targets (including the "blank", meaning no target). The details will not be given here, inasmuch as they can be developed easily by standard methods. When the polyethylene and carbon targets had equal stopping power, the carbon subtraction factor z was usually between 0.7 and 1.1.

Fig. 2 shows a plot of a typical set of data taken for fixed angles at various beam levels for both polyethylene and carbon targets. This type of graph lends itself well to the problem of separating the systematic coincidences from the accidental coincidences. The extrapolation to zero beam intensity gives the systematic coincidences. The slopes of the lines are due to accidental coincidences. The interpretation of the figure depends in our case on the assumptions that the cyclotron duty cycle is quite constant and the coincidence counting rates are small compared to the single crystal counting rates.

The effective resolving time was about 3×10^{-5} sec. The duty cycle corresponding to 60 pulses per second each 50×10^{-6} sec long was 3×10^{-3}. This gives an electronic resolving time of about 10^{-7} sec.

IV. TOTAL D-P SCATTERING CROSS SECTION

Deuteron-proton scattering, whether elastic or inelastic, results in two charged particles emerging from a collision. Moreover, conservation of energy and momentum require that no such particles emerge at (laboratory) angles greater than 90°. It is therefore sufficient, in finding the total cross section $\bar{\sigma}_{dp}$, to count the number of hydrogen scattered charged particles at various angles ϕ, integrate from 0 to $\pi/2$, and divide by two, inasmuch as we can count each scattering event twice.

$$\bar{\sigma}_{dp} = \pi \int_0^{\pi/2} \bar{\sigma}(\phi) \sin \phi \, d\phi. \qquad (2)$$

Here $\bar{\sigma}(\phi)$ is the complete charged particle differential scattering cross section as can be measured using a single charged particle counter, method B. The probability of counting the neutrons associated with the inelastic scattering events is quite small.

The results of this measurement are shown in Table I. Fig. 3 shows a plot of $\bar{\sigma}(\phi) \sin \phi$, together with the curve adopted for finding $\bar{\sigma}_{dp}$. It is clear that the elastic scattering cross section is infinite unless a cut-off is provided to exclude Rutherford scattering at small angles. The cut-off is made in this case by considering the elastic scattering to be zero for deflection angles of less than 10° in the c.m. system. This amounts to excluding the elastic scattering for laboratory angles smaller than 3.3° and greater than 85°. Fig. 3 shows discontinuities at these angles.

Some comment is necessary concerning the methods of obtaining $\bar{\sigma}(\phi)$ in different regions of angle. Between 3.3° and 70° method B (single counter) is used as described above. In the range of angles between 70° and 85° the charged particles (all protons) are of very low energy and many of them do not get out of the target, hence method B cannot be used. Since the inelastic scattering is expected to be very small in these angles the known elastic scattering is taken as the total scattering. For angles smaller than 3.3° we take no contribution from the elastic scattering and assume that the inelastic cross section is constant, so that $\bar{\sigma}(\phi) \sin \phi$ suffers a finite discontinuity at 3.3° and then passes linearly to the origin.

Table I. Total charged particle scattering from d-p collisions as a function of laboratory angle ϕ, obtained with method B. Errors quoted are r.m.s. counting errors.

ϕ degrees	$\pi \sin\phi\, \sigma(\phi)$, 10^{-27} cm^2 Date 4/16/51	Date 5/28/51	Elastic Scattering	Value used in integration
5		131±30		142
8	150±25	187±18		150
10		148±7		148
15	114±10	112±8		115
20		71±4		90
25	63±3	71±8		66
30		46±3		53
35	49±2			45
40		35±2		42
45	43±2	40±2		40
50		38±3		37
55	34±2			35
60		33±2		31
65	24±1	28±2	19±2	26
70		17±1	27±3	27
75	2±1	2±1	30±3	32
80		1±1		40
82	0		44±4	42
85				44

The resulting σ_{dp} is $(94^{+7}_{-5}) \times 10^{-27}$cm^2. This is to be compared with the total n-d cross sections of $(117\pm5) \times 10^{-27}$cm^2 and $(105\pm4) \times 10^{-27}$cm^2 obtained by Cook et al.[14] for 83 Mev neutrons, and DeJuren and Knable[15] for 95 Mev neutrons, respectively. The cross section obtained in the present work is evidently of the nature of a lower limit, since there is the question of how many particles could have been omitted from the regions 0 to 3.3 degrees and 70 to 90 degrees. This fact has supposedly been taken account in the assignment of errors, which are thus slightly unsymmetrical.

V. INELASTIC PROTON-PROTON TYPE SCATTERING

1. Kinematics and Geometry

The relative de Broglie wave length of deuteron and proton is much smaller than the average separation of the two nucleons inside the deuteron. It is therefore expected that most inelastic d-p collisions involve only two particles directly, the third particle going on almost undisturbed. We have looked for inelastic p-p type collisions, i.e. collisions in which the proton in the deuteron hits the target proton, causing the deuteron to break up and the neutron to remain virtually undisturbed. Method A was used. One counter, the "defining counter", was placed at angle ϕ to the beam. The position of the other crystal (at angle Θ) was varied over the surface of a sphere with the target as center, and by integration of the coincidences registered over all positions of this crystal (except that corresponding to elastic scattering) it was possible to obtain $\sigma_{pp}(\phi)$.

The kinematics can be calculated to good approximation by assuming that energy is conserved between all three particles, whereas momentum is conserved between only the two colliding ones, the momentum of the third particle remaining unchanged. Non-relativistically, in a free p-p collision, the angle $\Theta + \phi$ between two scattered particles must be $\pi/2$. It is not difficult to show that the effect of the 2 Mev binding energy of the deuteron is to shift $\Theta + \phi$ to a slightly lower value, to about 87° at $\phi = 20^\circ$, 88.7° at $\phi = 45^\circ$. Relativistic corrections lower the included angle by an additional amount of the order of 1°.

Qualitatively one may say that the internal momentum of the deuteron introduces a spread in the angular distribution of one proton relative to the other. Referring to Fig. 4 we may say that the angle $(\Theta + \phi)$ between the two out-going protons is not completely determined even if it is specified that one proton emerges at a definite angle ϕ with respect to the beam. Furthermore, the two outgoing protons and the beam are not in general coplanar. The horizontal spread in $(\Theta + \phi)$ is indicated in Fig. 4 by $\delta\Theta_1$. The vertical deviation of the second proton from the plane of the beam and the first proton is indicated by $\delta\Theta_2$. At first sight it would appear that these deviations $\delta\Theta_1$ and $\delta\Theta_2$ would both be of the order of (p_i/p_o), where p_i is the internal momentum of the deuteron and p_o is the momentum of the incident particle,

and indeed, this would be true if we were considering protons incident on a stationary deuteron. However, in this particular case of deuterons incident on protons, the horizontal spread $\delta\Theta_1$ is much smaller, being of the order of $(p_i/p_o)^2$. The vertical spread remains as expected of the order of p_i/p_o. These features are rather easily brought out by applying conservation of energy and momentum to the collision process with the added provision that the momentum of the unstruck particle (neutron) is unaffected in the collision.

These considerations are in agreement with experiment. One crystal was, for example, set at $\phi = 45^\circ$, and the other was set at a variable angle Θ in the scattering plane. Both crystals subtended approximately 4° at the target. The number of hydrogen counts per integrator volt is plotted in Fig. 5 as a function of $\phi + \Theta$. The elastic scattering peak, at $\phi + \Theta = 70.5^\circ$ (expected: 70.8°), is well resolved from the inelastic peak centered around 86.5°. The width of the inelastic peak is almost entirely due to the poor geometrical resolution as is evident from a comparison with the width of the elastic peak.

In practice, for purposes of finding a differential cross section, the crystal at angle Θ was made about 10° wide, and a curve of the type shown in Fig. 6 was obtained. It was then possible to operate at some point on the flat portion of the curve, say 86°, and raise and lower the Θ crystal to obtain the vertical distribution. The result of such a variation is shown in Fig. 7.

It was unnecessary to measure the height variation at every angle measured, for the total (integrated over height) hydrogen count $\underline{H}_t$ at some angle Θ corresponding to a defining crystal at ϕ could be determined from that at another angle Θ' corresponding to a defining crystal at ϕ' by the kinematic relationship

$$(\underline{H}_t/\underline{H}_o)_{\Theta} = (\underline{H}_t/\underline{H}_o)_{\Theta'} (\sin\phi'/\sin\phi), \qquad (3)$$

where $\underline{H}_o$ is the hydrogen count at zero height. This relation was checked to be in agreement with observation.

2. Sample Calculation.

We shall illustrate with a sample calculation of the cross section at $\phi = 45^\circ$, $\Theta = 41^\circ$. The cross section is, in general, given by

$$\sigma(\phi) = \frac{\underline{H}_t}{nN\Delta\Omega}, \qquad (4)$$

where $\Delta\Omega$ is the solid angle subtended at the target by the defining crystal at angle ϕ. N is the number of hydrogen atoms per cm^2 in the CH_2 target measured in the direction of the beam,

$$N = N_o \cdot \frac{2.016}{14.03} t, \qquad (5)$$

where t is the target surface density along the beam direction in g cm^{-2}, and N_o is Avagadro's Number. With $\underline{H}$ measured for 1 integrator volt, n is the number of incident deuterons required to charge a capacitance C_o connected to the collecting grid of the monitoring chamber to one volt. Thus

$$n = \frac{C_o}{e\mu} \qquad (6)$$

where e is the electronic charge in Coulombs, and μ the multiplication of the argon-filled chamber.* μ was 1806 at 20°C and a pressure of 77.8 cm Hg, the sensitive depth of the chamber being 5.11 cm.

A typical set of values at $\phi = 45°$, $\Theta = 41°$ was:

crystal at angle ϕ: area = 22.63 cm^2,
distance b from target = 95cm
solid angle = 0.00251

crystal at angle Θ: area = 36 cm^2
height h_o = 4.39 cm
distance c from target = 50cm
horizontal angular width: 10°

Targets were oriented perpendicular to the beam, and had surface densities

$\underline{CH_2}$: 0.283 g cm^{-2}
$\underline{C}$: 0.336 g cm^{-2}
$C_o = 0.102 \cdot 10^{-6}$ farad, integrating condenser including capacitance of cables.
Multiplication of chamber $\mu = 1806$
Resolving time $\tau = 1.5 \cdot 10^{-5}$ sec ± 10 percent.

The counts at h = 0 are summarized in Table II on the following page.

---

* There is no gas multiplication in these ionization chambers of the type used in proportional counters. Rather, the ratio of current in the ionization chamber to beam current is called the multiplication. Thus, one beam particle passing through the ionization chamber results in the collection of μ ion pairs.

Table II. Sample data for inelastic p-p type scattering at $\phi = 45^\circ$ $\Theta = 41^\circ$ (method A).

Target	Time, sec.	Total Counts ϕ	Θ	Coinc.	Integr. volts
CH_2	264	3231	18702	100	2.0
C	142	1439	8144	9	1.0
bl	63	302	1343	2	0.5

At these low counting rates it is not necessary to correct for counting losses in the scalers. Analysis of the accidental coincidences gives the carbon subtraction factor $z = 1.04 \pm 0.24$. Thus we obtain at $h = 0$ $\underline{H} = \underline{CH_2} - z\underline{C} - (1-z)\,\underline{bl} = 41 \pm 6$. Similarly we find $\underline{H}$ for other heights of the crystal at Θ. $\underline{H}_t$ is now found by integration under the curve of Fig. 7.

$$\underline{H}_t = \frac{1}{h_o} \int_{-\infty}^{\infty} \underline{H}\,dh = 132 \pm 13 \qquad (7)$$

where we assign a 10 percent error to $\underline{H}_t$. Thus we obtain

$N = 2.45 \cdot 10^{22}$ atoms cm^{-2},

$n = 3.53 \cdot 10^{8}$ deuterons per integrator volt, and

$\sigma(\phi) = (6.1 \pm 0.6) \cdot 10^{-27}$ cm^2.

3. Presentation of Data.

The inelastic cross sections at various angles ϕ are listed in Table III. The counting errors listed in Table III are estimates based on the possible variations in $\underline{H}_t$ within the statistical accuracies of the individual $\underline{H}$. Systematic errors (cf. Section VI) are included under the column marked total error. Values of $\sigma(\phi)$ marked with an asterisk are those for which the vertical distribution was calculated by means of Eq. (3) rather than measured. For $\phi = 30^\circ$ or 25° thin targets were used. Nevertheless at $\phi = 25^\circ$ the particles going into the corresponding angle $\Theta = 59^\circ$ have a range of only about 1/2 g/cm^2 of C, and it must therefore be assumed that due to energy spread caused by the internal motion in the deuteron a number of particles had insufficient range to produce a measurable pulse in the Θ crystal or were lost by multiple scattering. The positive error on the 25° datum should therefore be increased to perhaps 2 mb.

Table III. Summary of inelastic p-p type differential scattering cross sections in the laboratory as a function of laboratory angle ϕ. Figures of the last column include systematic errors of Section VI. Values marked with an asterisk* were calculated with help of Eq. (3).

Θ degrees	ϕ degrees	$\sigma(\phi)$ 10^{-27} cm^2/sterad	r.m.s. counting error 10^{-27} cm^2/sterad	r.m.s. total error 10^{-27} cm^2/sterad
59	25	6.3*	+ 2.0	+ 2.1
			- 1.2	- 1.4
55	30	7.3	± 0.6	± 0.9
48.5	37	6.0*	± 0.9	± 1.1
45	41	6.1	± 0.2	± 0.6
41	45	5.7	± 0.2	± 0.6
37	48.5	4.8*	± 0.7	± 0.9
30	55	4.5	± 0.4	± 0.6
25	59	3.1*	+ 1.0	+ 1.0
			- 0.6	- 0.7

Table III and Fig. 8 list the weighted mean cross sections. Note that the table can be extended to 59° inasmuch as $\sigma(\Theta) = \sigma(\phi) \sin\phi / \sin\Theta$. It should be emphasized that the values quoted in Table III for $\sigma(\phi)$ are lower bounds; if the proton distributions shown in Fig. 5 about $\theta + \phi = 86°$ and in Fig. 7 about h = 0 had long tails, these would almost surely escaped observation due to poor statistics, yet could contribute measurably to $\sigma(\phi)$.

VI. SOURCES OF ERROR

Following are some of the more important sources of error not previously mentioned:

1. Effective area of crystal faces. The actual area of the crystal surface is known in all cases to at least 2 percent. However, the crystal faces may not have been oriented perpendicularly to the incoming particles and the sensitivity of the crystals may not have been uniform across the surfaces. We believe the resulting error in the effective area of the crystal may have been as great as 3 percent.

2. Crystal Position. Possibly the largest source of error in the inelastic scattering data lay in the fact that the exact zero height position for crystals at angle Θ was not known. This uncertainty alone could produce an error of 7 percent. Uncertainties in the distance of the crystals from the target were of the order of 1 percent.

3. The polyethylene targets were analyzed and shown to be of composition $(CH_2)_n$ within 1 percent. The dimensions and weight, and hence the surface densities of the targets were known to 1 percent. Since all experiments were performed with the target perpendicular to the beam, errors due to non-perpendicularity at the target were negligible.

4. Multiple Scattering. Multiple scattering in the targets could have resulted in a loss of 2 percent of the events, except in the cases where one of the angles was greater than 60°, in which case, the loss may have amounted to as much as 5 percent.

5. Finite Coincidence Resolving Time. Losses due to finite resolving time of the coincidence circuit were negligible except in those cases where one of the crystals may have been close to the beam, in which case the high single counting rate from that crystal would produce errors of not more than 2 percent.

6. Carbon Subtraction. The method of finding z by measuring the single counting rates and the coincidence resolving time resulted in an uncertainty of not more than 2 percent due to possible variations of duty cycle that might have passed unnoticed.

7. Miscellaneous. Errors in the angle calibration of the scattering table and its alignment with the beam were not greater than 1 percent. The calibration of the ion chamber against the Faraday cup is believed accurate to 2 percent. The chamber was run at 1000 volts, high enough to measure better than 99 percent of the saturation current at any beam strength used.

Combining the sources of error just mentioned and those discussed in Sections IV and V, we may summarize by giving the systematic rms errors for the two experiments.

a) Total cross section: 5 percent.

b) Inelastic: 10 percent.

VII. CONCLUSION

The total cross section for neutron-deuteron scattering has been calculated by Chew[9] and by Gluckstern and Bethe.[10] The results can be taken over to proton-deuteron scattering if we assume charge independence of the nuclear forces. In the language of proton-deuteron scattering, the total cross section calculated by Chew is:

$$\sigma^t = (1 - \varepsilon)\,\sigma^t_{np} + \sigma^t_{pp} + I \qquad (8)$$

Where ε has been calculated by Chew to be 0.15 and I, the interference term, has been estimated by both Chew and Gluckstern and Bethe to be of the order of 15 mb. This calculation enables us to compare the experimentally observed total cross sections for n-p and p-p scattering, providing we take into account the small angle cut-off used to eliminate Coulomb effects. For σ^t_{np} we may take the entire total cross section as measured by DeJuren and Knable[15] of 73 mb. For the total p-p cross section we will assume a constant value of $d\sigma/d\omega$ of 3.97 mb/steradian in the center of mass. This figure is based on the measurements at 120 Mev of Chamberlain, Segrè, and Wiegand[4*] and is integrated for angles greater than 10^o, thus preserving a cut-off which agrees with that used in our own calculations. The total p-p cross section calculated on this basis is 25 mb. Therefore the theoretical cross section for d-p scattering is $\sigma^t = 0.85 \times 73 + 25 + 15 = 102$ mb. This figure should be compared with our experimental value of (94^{+7}_{-5}) mb.

The differential cross section for inelastic p-p type collisions may be compared with the free p-p cross sections at comparable energies. Comparison with the results of Chamberlain, Segrè and Wiegand[4] taken in the laboratory frame of reference, indicates that our inelastic p-p type cross section is approximately half the free p-p cross section. This is somewhat less than has been expected theoretically. If we wish to consider the total cross section for this process, we observe that this is also the cross section for production of neutrons with little change in momentum. Transferring

---

* Discrepancies in the differential proton-proton scattering cross sections obtained at Berkeley and elsewhere are believed to be due to different methods of beam integration. For this reason we prefer, at the present time, to compare our results with those of the Berkeley group, even though the comparable energies are somewhat higher, because these measurements employ the same beam integration methods as are used in our experiments and therefore allow a direct comparison.

again to a system in which neutrons are incident on deuterons, as is employed by Chew[9], we find that we must compare with the total cross section for production of slow protons. This cross section is given by Chew as $6^{t}_{slow} = 0.58 \times 6^{t}_{nn}$. However, it must be pointed out that the inelastic p-p type cross section must deviate considerably from a fixed ratio with the free p-p cross section, at small and large angles, since small momentum transfers will favor elastic collisions. Therefore, it would appear that theoretically we should expect the inelastic type collision to be perhaps 0.7 times the free cross section, rather than 0.5 as is observed. Part of this discrepancy may be explained by the fact that we could not observe low energy particles.

We wish to thank Prof. E. Segrè and Dr. Martin O. Stern for their assistance and encouragement, and the crew of the 184-inch cyclotron for their cooperation during the experiments.

REFERENCES

1. J. Hadley, E. Kelly, C. Leith, E. Segrè, C. Wiegand and H. York, Phys. Rev. 75, 351 (1949).
2. R. Birge, U. Kruse and N. Ramsey, Phys. Rev. 83, 274 (1951).
3. C. Oxley and R. Schamberger, Phys. Rev. 85, 416 (1952).
4. O. Chamberlain, E. Segrè, C. Wiegand, Phys. Rev. 83, 923 (1951).
5. J. Cassels, G. Stafford and T. Pickavance, Nature 168, 468 (1951).
6. T. Wu and J. Ashkin, Phys. Rev. 73, 986 (1951).
7. G. F. Chew, Phys. Rev. 74, 809 (1948).
8. G. F. Chew, Phys. Rev. 80, 196 (1950).
9. G. F. Chew, Phys. Rev. 84, 710 (1951).
10. R. L. Gluckstern and H. A. Bethe, Phys. Rev. 81, 761 (1951).
11. M. Stern and O. Chamberlain, Phys. Rev. (to be published).
12. W. Aron, B. Hoffman, and F. Williams - Range-Energy Curves, AECU-663 (UCRL-121 2nd rev.) unpublished.
13. C. Wiegand, Rev. Sci. Inst. 21, 975 (1950).
14. L. Cook, E. McMillan, J. Peterson and D. Sewell, Phys. Rev. 75, 7 (1949).
15. J. DeJuren and N. Knable, Phys. Rev. 77, 606 (1950).

FIGURE CAPTIONS

Fig. 1 Block diagram of the electronic circuits of the experiment (as used in method A of the text) together with a schematic top view of the coincidence apparatus.

Fig. 2 Coincidence counts per unit beam charge plotted as a function of beam current for CH_2 and C targets. The ratio of CH_2 slope to C slope determines approximately the carbon subtraction factor z, here about 1.1.

Fig. 3 Differential d-p scattering cross section for all charged particles as obtained with method B. The quantity $\pi \sin\phi\, \sigma(\phi)$ in mb sterad.$^{-1}$ is shown as a function of scattering angle ϕ. The discontinuities at 3.3° and 85° are due to the cut-off of the elastic scattering. The area under this curve is proportional to the total d-p scattering cross section.

Fig. 4 Geometry of inelastic p-p type scattering as studied using method A, showing the angles ϕ and Θ relative to the beam and the contours of equal coincidence counting rate. $\delta\Theta_1$ is a measure of the horizontal spread, $\delta\Theta_2$ a measure of the vertical spread.

Fig. 5 Coincidence counting rate due to hydrogen plotted as a function of the angle between the counters. The large peak is from elastic scattering; the smaller one from inelastic p-p type scattering. The angle subtended horizontally by each crystal was approximately 4°.

Fig. 6 Coincidence rate due to inelastic p-p type scattering as a function of the angle between crystals, at $\phi = 45^\circ$. The angle subtended horizontally by the Θ crystal is approximately 10°.

Fig. 7 p-p type inelastic scattering effect as a function of the height of the Θ crystal; $\phi = 45^\circ$, $h_o = 4.4$ cm, the Θ crystal is 50 cm from the target, and $\phi + \Theta = 86^\circ$.

Fig. 8 Inelastic p-p type differential scattering cross section, obtained with method A, plotted as a function of the (lab.) scattering angle ϕ. Errors shown are total r.m.s. errors.

UCRL-2237
Unclassified-Physics Distribution

UNIVERSITY OF CALIFORNIA

Radiation Laboratory

Contract No. W-7405-eng-48

SCATTERING OF 190-MEV DEUTERONS ON PROTONS

Arnold L. Bloom and Owen Chamberlain

June 4, 1953

Berkeley, California

UCRL-2237
Unclassified-Physics Distribution

SCATTERING OF 190-MEV DEUTERONS ON PROTONS

Arnold L. Bloom and Owen Chamberlain

Radiation Laboratory, Department of Physics,
University of California, Berkeley, California

June 4, 1953

ABSTRACT

A measurement of the total d-p scattering cross section is reported. Because of the divergence of coulomb scattering at small angles a small angle cut-off has been applied to the elastic scattering. The result may be stated as follows: The cross section for elastic scattering to angles greater than 10 degrees in the c.m. system, plus the total inelastic scattering cross section is $(94\ ^{+7}_{-5}) \times 10^{-27}$ cm^2.

Measurements are also reported of those inelastic scattering processes in which both protons suffer significant momentum changes. We have termed these events "inelastic p-p type collisions". The differential cross sections for these events appear to be smaller than would be expected in view of the theoretical considerations of others.

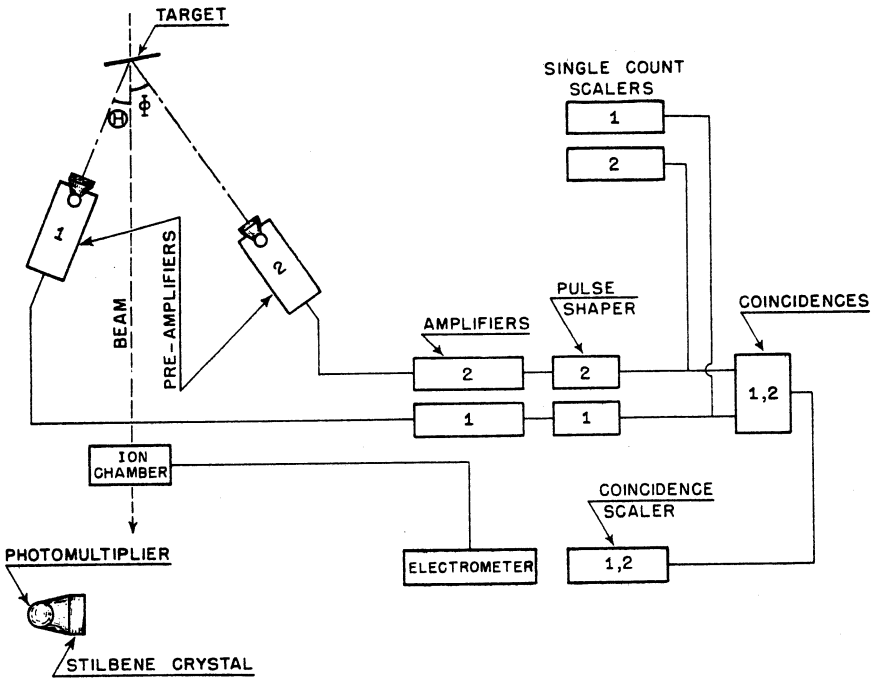
TARGET
SINGLE COUNT SCALERS
1
2
1
2
BEAM
PRE-AMPLIFIERS
PULSE SHAPER
AMPLIFIERS
COINCIDENCES
2
2
1,2
1
1
ION CHAMBER
COINCIDENCE SCALER
PHOTOMULTIPLIER
ELECTROMETER
1,2
STILBENE CRYSTAL
MU-5213

Fig. 1

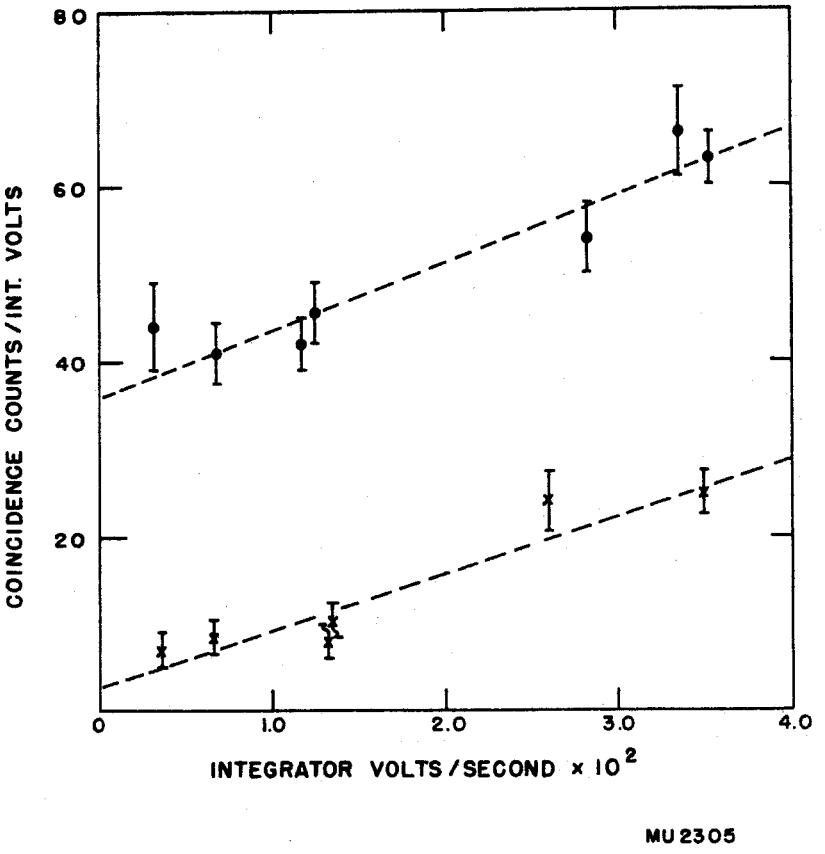
80
60
40
20
0
1.0
2.0
3.0
4.0
COINCIDENCE COUNTS / INT. VOLTS
INTEGRATOR VOLTS / SECOND x 10 2
MU 2305

Fig. 2

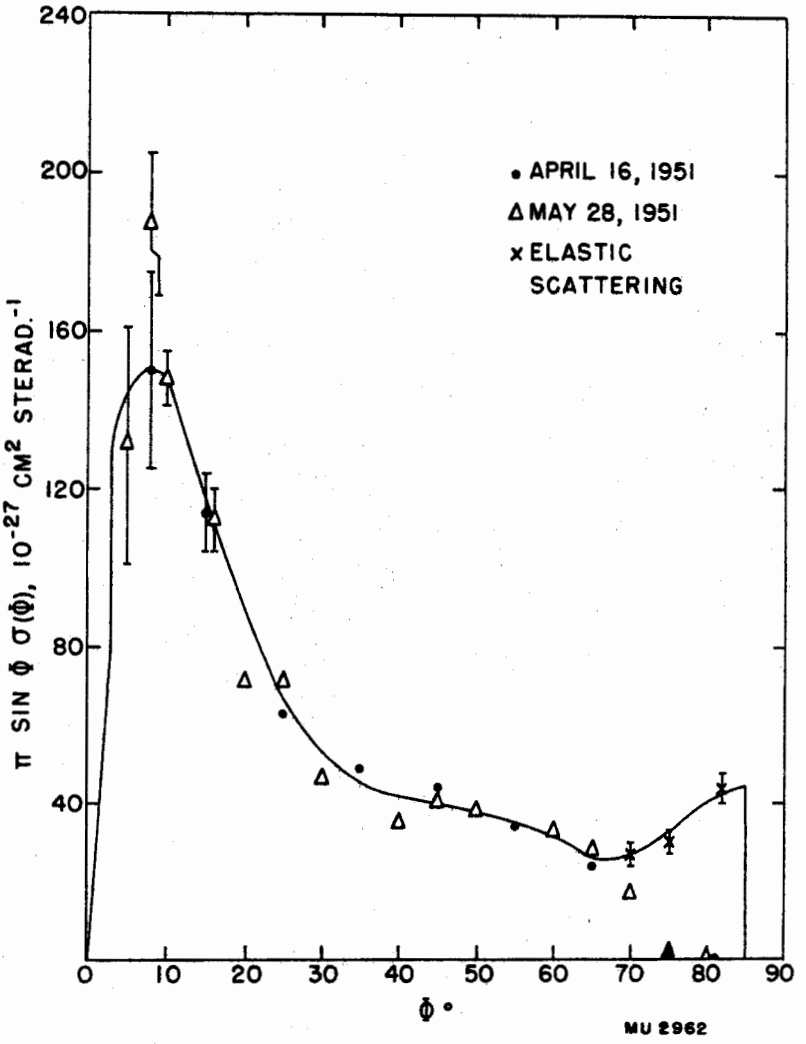
240
200
160
120
80
40
0
10
20
30
40
50
60
70
80
90
Φ°
π SIN Φ σ(Φ), 10⁻²⁷ CM² STERAD.⁻¹
• APRIL 16, 1951
Δ MAY 28, 1951
x ELASTIC SCATTERING
MU 2962

Fig. 3

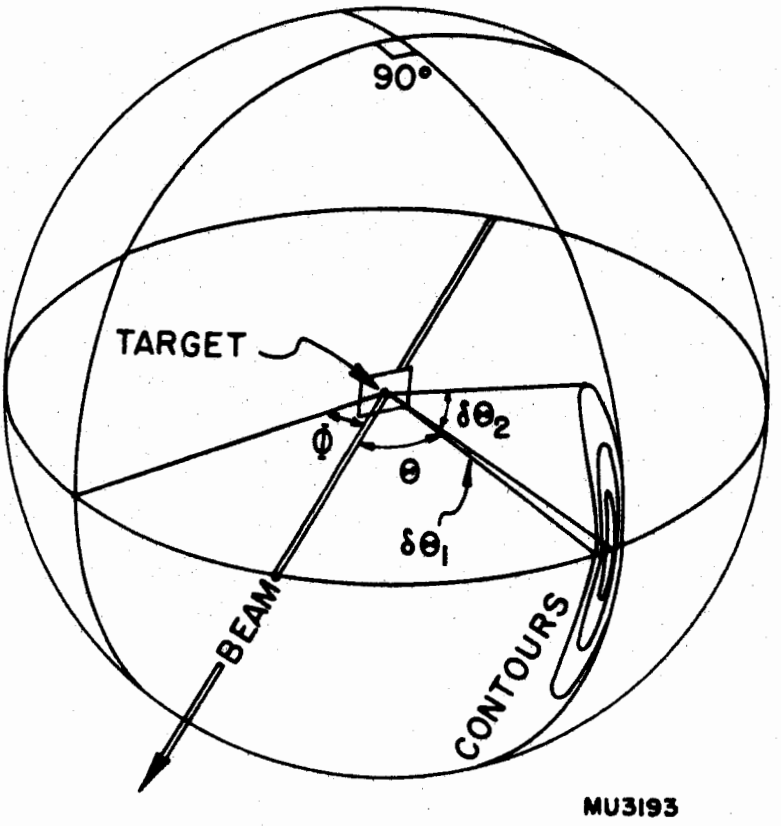

Fig. 4

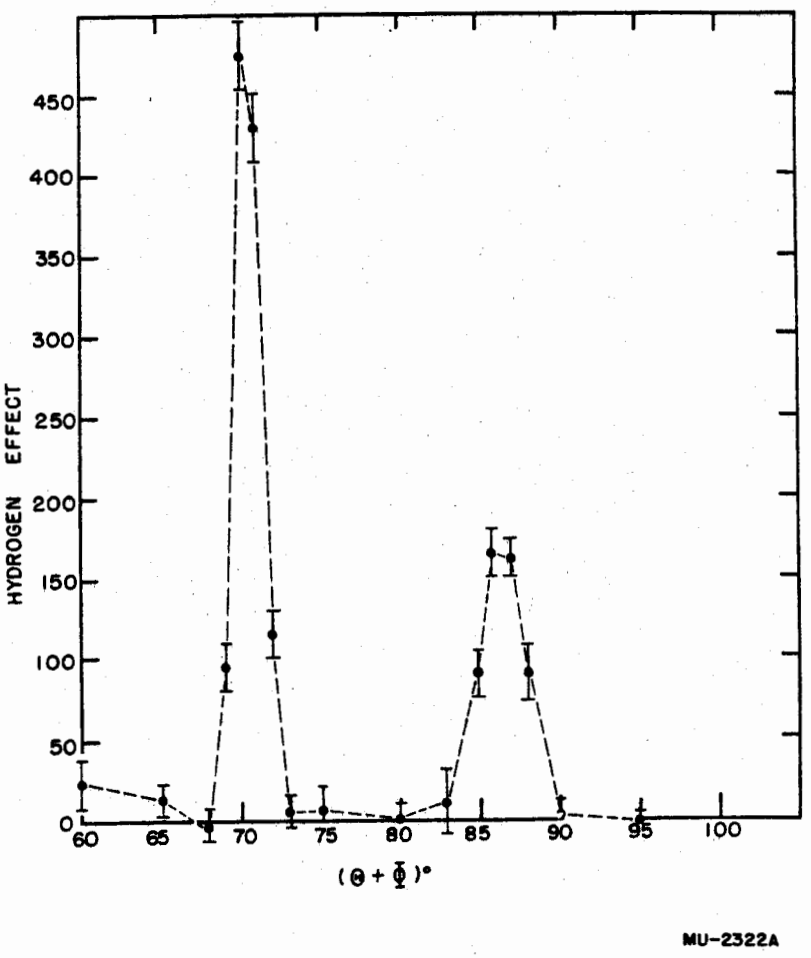
HYDROGEN EFFECT
450
400
350
300
250
200
150
100
50
0
60
65
70
75
80
85
90
95
100
(Θ + Φ)°
MU-2322A

Fig. 5

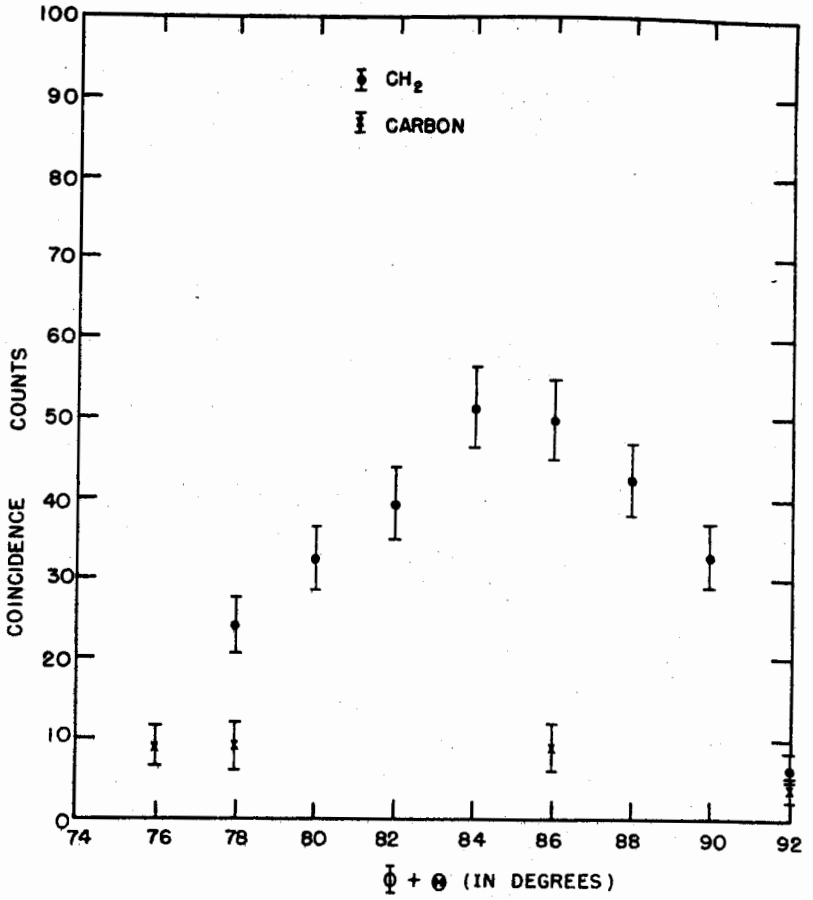
CH2
CARBON
COINCIDENCE COUNTS
100
90
80
70
60
50
40
30
20
10
0
74
76
78
80
82
84
86
88
90
92
Φ + Θ (IN DEGREES)
MU-2323A

Fig. 6

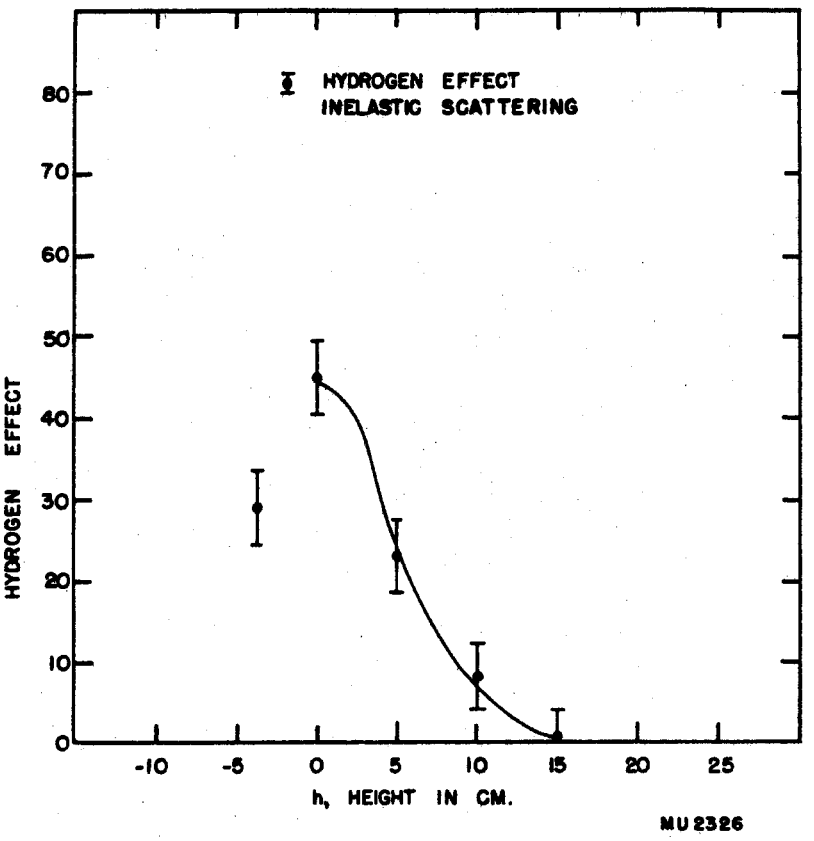
HYDROGEN EFFECT
INELASTIC SCATTERING
HYDROGEN EFFECT
80
70
60
50
40
30
20
10
0
-10
-5
0
5
10
15
20
25
h, HEIGHT IN CM.
MU 2326

Fig. 7

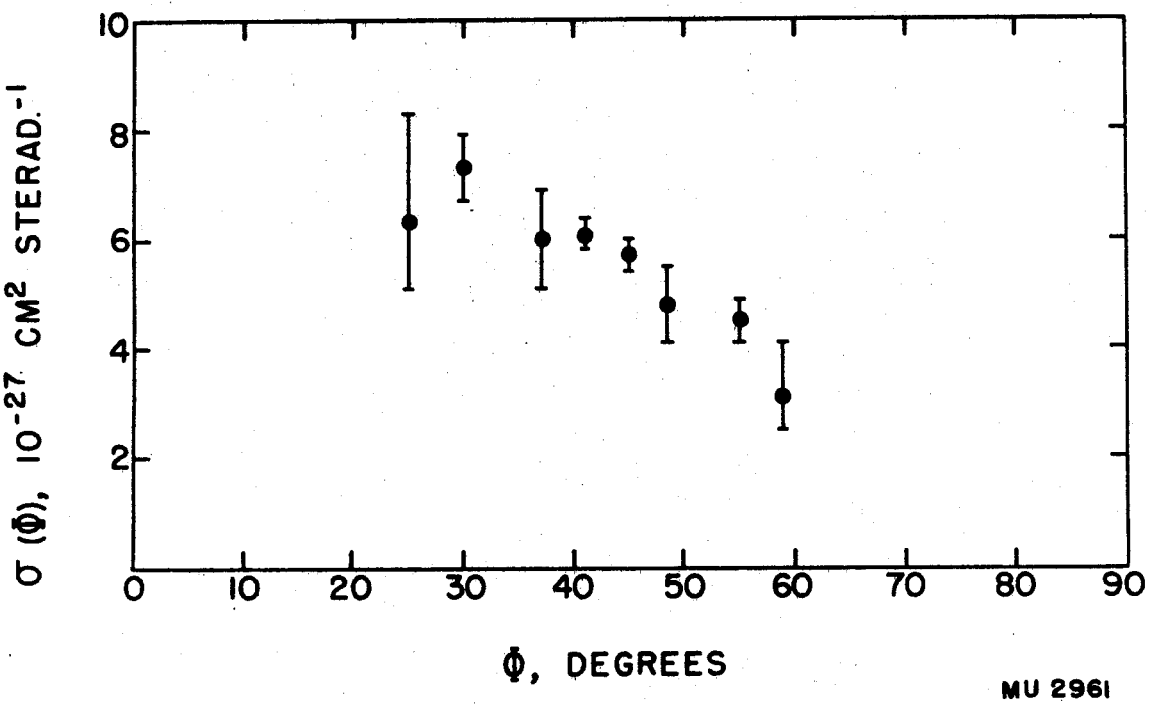
10
8
6
4
2
0
10
20
30
40
50
60
70
80
90
σ (Φ), 10-27 CM2 STERAD.-1
Φ, DEGREES
MU 2961

Fig. 8